Journal of Engineering Research Innovation and Scientific Development 3 (2), (2025), 30-36 https://doi.org/10.61448/jerisd32256

Journal of Engineering Research Innovation and Scientific Development
journal homepage: www.jerisddelsu.com
Print ISSN 2971-6594 Online ISSN 2971-6608

Model for Inclusive Pressure Distribution of Horizontal Well in a Two-Layered Bounded Extended Reservoir

M.C. Ogbue*[1], K. Ezewu[2], J.O. Eyenubo[3], E.E. Ebisine[4], F.E. Olokpa[5], S.E. Adewole[6], K.O. Bello[7]

[1]Department of Petroleum Engineering, Delta State University, Abraka, Nigeria
[2]Department of Mechanical Engineering, Delta State University, Abraka, Nigeria
[3-5]Department of Electrical Engineering, Delta State University, Abraka, Nigeria
[6-7]Department of Petroleum Engineering, University of Benin, Benin City, Nigeria

Corresponding author: mogbue@delsu.edu.ng (*Ogbue M.C)

Article history: Received: 02-03-25, Revised: 02-06-25, Accepted: 08-06-25, Published: 10-06-25

Abstract

Growing applications of horizontal well technology warrant attempts towards modelling for more realistic phenomena. In the study of performance of horizontal wells in layered reservoirs, particular issues have been dealt with; however, existing models restrict the number of flow regimes. In this research, the pressure distribution of horizontal wells in layered reservoirs was presented in the form of dimensionless pressure and dimensionless pressure derivative functions of reservoir system properties and fluid properties without restriction on the number and type of flow regimes. The model considered the effect of the interface on pressure response and the effect of crossflow. From the results obtained, dimensionless pressure depends on the type of interface, degree of crossflow, dimension of layer, regional well parameters, and regional rock and fluid properties. Dimensionless pressure was found to increase as the degree of crossflow reduces. Dimensionless pressure decreases as layer thickness increases. The type, interval of subsistence, and number of existing flow regimes depend largely on the reservoir system parameter, the location of the interface relative to the well, and the degree of crossflow. A horizontal well in a bound layered reservoir experiences a minimum of eleven (11) flow regimes, including some transition periods at full flow, i.e., when all the external boundaries are felt. During a flow period, the type and number of flow regimes that may occur, as well as the duration of existence, are determined by the values of parameters, the geometry of the reservoir, the fluid properties and the well architecture selected. The model was seen to produce a series of radial and linear flows along the individual principal axes or combinations of any of the three principal axes. Each flow regime could be recognised by its characteristic signature in the log-log graph plots of the pressure and pressure derivative versus time. Flexibility of the model in this article allows for an easy switch of reservoir features between isotropy and anisotropy, single compartment and layered, and homogeneity and heterogeneity.

Keywords: Horizontal well; layered reservoir; pressure distribution model; unlimited number of flow regimes

1. Introduction

A recent development in technology has given impetus to questioning the suitability of existing models, relaxing some simplifying assumptions used in deriving existing models and exploring more realistic conditions in models for pressure distribution of wells in reservoirs. Too many simplifying assumptions in deriving models actually create a wide gap between natural phenomena and the models for such phenomena. For instance, literature usually considers six of five flow regimes as the possible flow regimes in reservoirs produced by horizontal wells (Odeh *et al.,* 1990; Kuchuk *et al*., 1996; Du *et al*., 1992; Al Rbeawi *et al*., 2013). However, research reveals that the number of possible flow regimes could be more. When models derived on the premise of fewer flow regimes are used to derive well test analysis procedures, the interpretation model will not have the capability to interpret certain information communicated by the reservoir system. Another limiting assumption relates to the homogeneity and isotropy of the reservoir. Geological models derived from real data reveal those reservoirs as heterogeneous and anisotropic. For instance, a reservoir assumed to be a single compartment may actually be an extended reservoir, such as a double-layered reservoir having a cross-flow interface. As a result, some information communicated in the form of data points from the well test may be treated as noise and thus ignored because of limitations in the model.

Recent literature is still replete with researches on pressure distribution of horizontal wells with limited flow regimes (Afagwu et al., 2020; Chen et al., 2016; Al Rbeawi *et al*., 2013; Oloro *et al*., 2012; Owolabi *et al*., 2012; Adewole *et al*., 2012). Some of these researchers study the performance of horizontal wells in a single-compartment reservoir while providing for certain requirements. For instance, transient flow behaviour (Mutisya *et al.,* 2020) and multi-boundary systems (A1 Rbeawi *et al*., 2013). Other researchers extended the study of the performance of horizontal wells to layered reservoirs while providing for certain requirements. For instance, simultaneous gas cap and bottom water drives (Oloro *et al*., 2012). Early research works have shown that for homogenous reservoirs, linear flow should be the dominant flow regime when well length is large compared to reservoir thickness (Du *et al*., 1992). In the log-log derivative diagnostic plot, a half slope would frequently be exhibited. It was also observed that the linear flow region gives a quarter slope line, "bilinear flow". Pressure distribution of horizontal wells in a layered reservoir with crossflow has been shown to be the same as that of the homogenous system (Oloro *et al*., 2012). Therefore, pressure responses in a crossflow reservoir would be higher than that without crossflow. Basically, these articles were published in the late 1990s and very early 2010s. They provided the fundamental knowledge upon which the study of horizontal wells and layered reservoir models will be derived, as can be seen in most recent works. Recent research works have shown that the flow regimes of multiple horizontal fractures, compared to the case of a single horizontal fracture, have two new peculiar flow regimes (Chu *et al*., 2019). A new analytical solution to the pressure transient behaviour for a uniform flux with a fully penetrating vertical well in a multilayer reservoir with formation crossflow shows that the dimensionless crossflow coefficient is a function of the time and distance from the wellbore. It was shown that when producing time is sufficiently long, crossflow will cease to exist and crossflow coefficients will be equal to zero, thus suggesting that there are no effects of adjacent layers on the pressure drop of each layer. These findings indicate that each layer produces independently (Lu *et al*., 2021). Articles on heterogeneous reservoirs with multiple-fractured horizontal wells have shown that the fluid flow around fracture ends exhibits non-linear flow. A semi-analytical model for multiple-fractured horizontal wells in heterogeneous reservoirs was derived using the source function with the boundary element method (Wang *et al*., 2017).

However, existing models have a restricted number of flow regimes possible for a horizontal well in a reservoir. Therefore, a good number of flow regimes during the intermediate flow time were not considered. An assessment of a layered reservoir as a function of both fluid and rock properties suggests the geological reality of the reservoir. In such a context, more possible flow regimes of the reservoir system can be revealed. In this article, the pressure distribution model for more possible flow regimes was studied. Flow dynamics at the cross-flow interface, which is also a common geological feature, was also put into consideration.

2. Materials and Method

A conceptual model is developed from which a physical model and subsequent mathematical model were derived. Flow regimes were delineated. Input data was processed. Pressure distribution was generated from a mathematical model followed by analyses of pressure distribution.

2.1 Conceptual Model

Consider a reservoir split into two layers of different petrophysical properties by a permeable interface. The characteristic feature of a crossflow interface is its capacity to allow seepage of fluid from one layer to the other. Crossflow causes changes in the pressure response of the well. The effect of the interface on pressure is represented by individual layer factors A and B.

2.2 Physical Model

The physical model is presented in Figure 1 as a 2D reservoir.

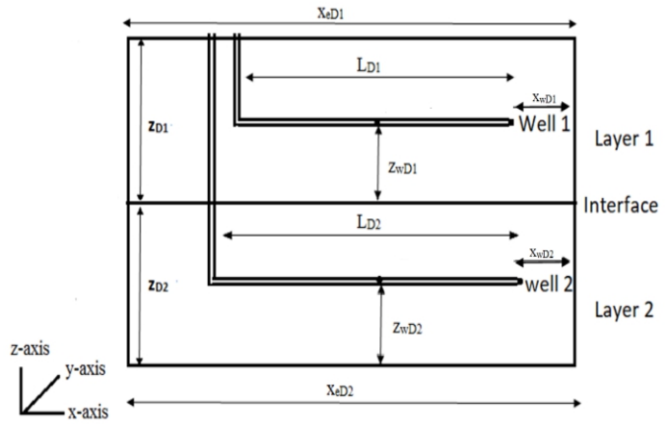

Figure 1: Physical model presented as 2D Layered Reservoir

The three principal axes of flow are designated as the x-axis, y-axis and z-axis. These three axes represent the major axes of permeability where, k_x, k_y and k_z are permeability along x-axis, z-axis and z-axis respectively. The anisotropy is defined such that, $k_x > k_y > k_z$. Heterogeneity is defined such that $\emptyset_1 \neq \emptyset_2$ where $\emptyset_1$ and $\emptyset_2$ are porosity values of layer 1 and layer 2 respectively. Also, heterogeneity is defined such that $C_{t1} \neq C_{t2}$ where C_{t1} and C_{t2} are total compressibility values of layer 1 and layer 2 respectively.

Assumptions:

i. The reservoir is horizontal, with uniform thickness, and all external boundaries are closed.

ii. Properties are uniform within an individual layer but different from the properties of other layers.

iii. Single-phase fluid flows from the reservoir to the well at a constant rate.

iv. Interface extends the entire length of the reservoir.

v. Properties of the interface are uniform along its entire length.

2.3 Possible Flow Regime and Types

Here for clarity, the flow regimes of a horizontal well with a single layer are reviewed, described and demarcated. The wellbore storage and skin factor are not considered; hence, the wellbore storage coefficient and the skin factor equal zero. A list of possible flow regimes with descriptions of their flow patterns, conditions of existence and intervals of existence is presented in Table 1.

Each flow regime can be identified mathematically by two peculiarities: (1) its source function and (2) its interval of existence (used as limits of integration). No two types of flow regimes have exactly the same function and limits of integration. It is pertinent to make clear that the number assigned to the time interval was arbitrarily done. It does not suggest the order in which they would exist.

2.4 Mathematical Model

The mathematical model is in the form of dimensionless pressure and dimensionless pressure derivative as functions of reservoir system parameters and fluid properties. Mathematical model was derived employing instantaneous source term and Green's function proposed for constant-rate model (Gringarten et al 1973). The model showed approximate solutions corresponding to the appropriate time limits.

2.4.1. Mathematical Axial Description

Reservoir description along each of the axis was properly described so as the know the appropriate function to select.

i. Reservoir description along x- axis:

a. The reservoir is sealed at the ends. Prescribed flux boundary condition.

b. The well length coincides with the x-axis

c. Therefore, the well is an infinite slab source in an infinite slab reservoir, represented by source number x (x).

Physical description is as shown in Figure 2.

Figure 2: Physical axial description of reservoir along x-axis

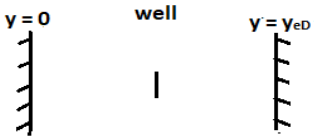

Figure 3: Physical description for y-axis

ii. Reservoir description along the y-axis:

a. The reservoir is sealed at both ends. Prescribed influx boundary condition.

b. The well length does not coincide with the y-axis.

c. Therefore, the well is an infinite plane source in an infinite slab reservoir, represented by source number vii(y).

Physical description is as shown in Figure 3.

i. Reservoir description along z-axis:

Layer 1

a. The reservoir is sealed at the top and has a constant pressure boundary (interface) at the bottom. This is a "mixed boundaries condition".

b. The well length does not coincide with the z-axis.

c. Therefore, the well is an infinite plane source in an infinite slab reservoir, represented by the modified form of source number ix (z) written as ix (z).

This function, ix (z)', is an extension of the existing source function for mixed boundaries, having prescribed pressure at the top and prescribed flux at the bottom.

Physical description is as shown in Figure 4a.

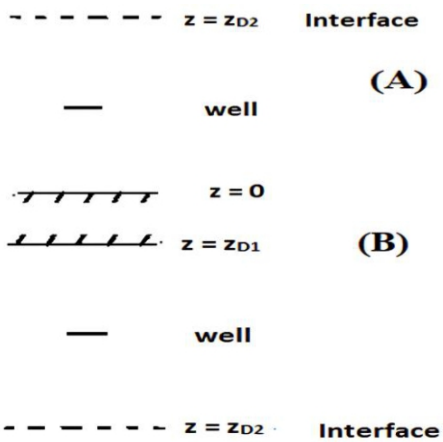

Figure 4: Physical description for z-axis. (A) Layer 1 (B) Layer 2

Table 1: List of possible flow regimes with descriptions of their flow patterns, conditions of existence and intervals of existence

Designation	Description of Flow Pattern	Condition of Existence	Interval of Existence
1	Flow along y, z-axes.	Flow is not beyond tip of well	0 - t_{D1}
2	Flow along x, y, z-axes	Flow is beyond tip of well.	$t_{D2} - t_{D3}$
3(a)	Flow along y-axis	Boundary along the z-axis is closest to well	$t_{D4} - t_{D5}$
3(b)	Flow along z-axis.	Boundary along the y-axis is closest to well	$t_{D6} - t_{D7}$
4(a)	Flow along x, y-axes	Given 3a existed	$t_{D8} - t_{D9}$
4(b)	Flow along x, z-axes	Given 3b existed	$t_{D8} - t_{D10}$
4(c)	Flow along y, z–axes	Given 2 existed	$t_{D8} - t_{D11}$
5(a)	Flow along y-axis	Given 4a or 4c existed	$t_{D12} - t_{D13}$
5(b)	Flow along z-axis	Given 4b or 4c existed	$t_{D14} - t_{D15}$
5(c)	Flow along x-axis	Given 4a or 4b existed	$t_{D16} - t_{D17}$
6	Flow along x, y, z-axes	All boundaries felt	$t_{D17} - t_{D18}$

Layer 2

a. The reservoir is sealed at the bottom and has a constant pressure boundary (interface) at the top. This is a "mixed boundaries condition".
b. The well length does not coincide with the z-axis.
c. Therefore, the well is an infinite plane source in an infinite slab reservoir, represented by source number ix (z). This is the source function for a mixed boundary having prescribed pressure at the bottom and prescribed flux at the top. Physical description is as shown in Figure 4b.

2.4.2 Dimension Pressure Expression

From the physical and mathematical description, expressions are written down for dimensionless pressure according to the Newman product rule:

Layer 1

$$P_{D1} = 2\pi h_{D1} A \int_0^{t_D} x(x).\, vii\,(y).\, ix\,(z)'\, d\tau \quad (1)$$

Equation 1 is the late-time expression for layer 1, when all the boundaries have been felt. Before late time, a series of flow regimes occur such that at any time, dimensionless pressure at any time of interest is a time superimposition of individual flow regimes that have existed up to the time of interest. Each flow regime is represented by an integrand, and the interval of existence is represented by the limits of the integration. Each integrand contains the source and Green's function of the three axes applicable to that flow period (Gringarten *et al.,* 1973). So, Equation 1 can be expressed as shown in Equation 2 for all possible flow regimes written above.

$$\begin{aligned} P_{D1} = {} & 2\pi h_{D1} \int_0^{t_D} ii(x).\, i\,(y).\, i\,(z) d\tau + 2\pi h_{D1} \int_{t_{D2}}^{t_{D3}} ii(x).\, i\,(y).\, i\,(z) d\tau + \\ & 2\pi h_{D1} A \int_{t_{D4}}^{t_{D5}} ii(x).\, i\,(y).\, ix\,(z)'\, d\tau + 2\pi h_{D1} \int_{t_{D6}}^{t_{D7}} ii(x).\, vii\,(y).\, i\,(z) d\tau + \\ & 2\pi h_{D1} A \int_{t_{D8}}^{t_{D9}} ii(x).\, i\,(y).\, ix\,(z)'\, d\tau + 2\pi h_{D1} \int_{t_{D8}}^{t_{D10}} ii(x).\, vii\,(y).\, i\,(z) d\tau + \\ & 2\pi h_{D1} \int_{t_{D8}}^{t_{D11}} ii(x).\, i\,(y).\, i\,(z) d\tau + 2\pi h_{D1} A \int_{t_{D12}}^{t_{D13}} ii(x).\, i\,(y).\, ix\,(z)'\, d\tau + \\ & 2\pi h_{D1} \int_{t_{D2}}^{t_{D3}} ii(x).\, i\,(y).\, i\,(z) d\tau + 2\pi h_{D1} \int_{t_{D14}}^{t_{D15}} x(x).\, vii\,(y).\, i\,(z) d\tau + \\ & 2\pi h_{D1} A \int_{t_{D16}}^{t_{D17}} ii(x).\, vii\,(y).\, ix\,(z)'\, d\tau + 2\pi h_{D1} A \int_{t_{D18}}^{t_{D19}} x(x).\, vii\,(y).\, ix\,(z)'\, d\tau + \end{aligned} \quad (2)$$

And the dimensionless pressure derivative as shown in Equation 3 and 4

$$P'_{D1} = \frac{\partial P_{D1}}{\partial int_D} \quad (3)$$

$$\begin{aligned} P'_{D1} = {} & 2\pi h_{D1} [ii(x).\, i\,(y).\, i\,(z)] + 2\pi h_{D1} [ii(x).\, i\,(y).\, i\,(z)] + \\ & 2\pi h_{D1} A [ii(x).\, i\,(y).\, ix\,(z)'] + 2\pi h_{D1} [ii(x).\, vii\,(y).\, i\,(z)] + \\ & 2\pi h_{D1} A [ii(x).\, i\,(y).\, ix\,(z)'] + 2\pi h_{D1} [ii(x).\, vii\,(y).\, i\,(z)] + \\ & 2\pi h_{D1} [x(x).\, i\,(y).\, i\,(z)] + 2\pi h_{D1} A [x(x).\, i\,(y).\, ix\,(z)'] + \\ & 2\pi h_{D1} [ii(x).\, i\,(y).\, i\,(z)] + 2\pi h_{D1} [x(x).\, viii\,(y).\, i\,(z)] + \\ & 2\pi h_{D1} A [ii(x).\, vii\,(y).\, ix\,(z)'] + 2\pi h_{D1} A [x(x).\, viii\,(y).\, ix\,(z)'] \end{aligned} \quad (4)$$

Constant A is only applicable to flow regimes that have felt the interface as one of their boundaries. Therefore, if the interface is not felt, the constant A is not included in the integrand representing the flow regime.

Layer 2

Similarly, the dimensionless pressure for Layer 2 is written as follows for late time.

$$P_{D2} = 2\pi h_{D2} B \int_0^{\alpha t_D} x(x).\, vii\,(y).\, ix\,(z)\, d\tau \quad (5)$$

Equation 5 is the late-time expression for layer 2, when all the boundaries have been felt. Before late time, a series of flow regimes occur, such that at any given moment, the dimensionless pressure is a time superposition of the individual flow regimes that have existed up to that point. Each flow regime is represented by an integrand, and its interval of existence is represented by the limits of integration. Each integrand contains the source and Green's functions corresponding to the three axes applicable to that flow period (Gringarten et al., 1973). Equation 5 can be expressed as shown in Equation 6 for all possible flow regimes. The dimensionless pressure derivative is presented in Equations 7 and 8.

$$\begin{aligned} P_{D2} = {} & 2\pi h_{D2} \int_0^{\alpha t_{D1}} ii(x).\, i\,(y).\, i\,(z) d\tau + 2\pi h_{D2} \int_{\alpha t_{D2}}^{\alpha t_{D3}} ii(x).\, i\,(y).\, i\,(z) d\tau + \\ & 2\pi h_{D2} B \int_{\alpha t_{D4}}^{\alpha t_{D5}} ii(x).\, i\,(y).\, I\,(z)\, d\tau + 2\pi h_{D2} \int_{\alpha t_{D6}}^{\alpha t_{D7}} ii(x).\, vii\,(y).\, i\,(z) d\tau + \\ & 2\pi h_{D2} B \int_{\alpha t_{D8}}^{\alpha t_{D9}} ii(x).\, i\,(y).\, I\,(z)\, d\tau + 2\pi h_{D2} \int_{\alpha t_{D8}}^{\alpha t_{D10}} ii(x).\, vii\,(y).\, i\,(z) d\tau + \\ & 2\pi h_{D2} \int_{\alpha t_{D8}}^{\alpha t_{D11}} ii(x).\, i\,(y).\, i\,(z) d\tau + 2\pi h_{D2} B \int_{\alpha t_{D12}}^{\alpha t_{D13}} ii(x).\, i\,(y).\, ix\,(z)\, d\tau + \\ & 2\pi h_{D2} \int_{\alpha t_{D2}}^{\alpha t_{D3}} ii(x).\, i\,(y).\, i\,(z) d\tau + 2\pi h_{D2} \int_{\alpha t_{D14}}^{\alpha t_{D15}} x(x).\, vii\,(y).\, i\,(z) d\tau + \\ & 2\pi h_{D2} B \int_{\alpha t_{D16}}^{\alpha t_{D17}} ii(x).\, vii\,(y).\, ix\,(z)\, d\tau + 2\pi h_{D2} B \int_{\alpha t_{D18}}^{\alpha t_{D19}} x(x).\, vii\,(y).\, ix\,(z)\, d\tau \end{aligned} \quad (6)$$

$$P'_{D2} = \frac{\partial P_{D2}}{\partial in \alpha t_D} \quad (7)$$

$$\begin{aligned} P'_{D2} = {} & 2\pi h_{D2} [ii(x).\, i\,(y).\, i\,(z)] + 2\pi h_{D2} [ii(x).\, i\,(y).\, i\,(z)] + \\ & 2\pi h_{D2} B [ii(x).\, i\,(y).\, ix\,(z)] + 2\pi h_{D2} [ii(x).\, vii\,(y).\, i\,(z)] + \\ & 2\pi h_{D2} B [ii(x).\, i\,(y).\, ix\,(z)] + 2\pi h_{D2} [ii(x).\, vii\,(y).\, i\,(z)] + \\ & 2\pi h_{D2} [x(x).\, i\,(y).\, i\,(z)] + 2\pi h_{D2} B [x(x).\, i\,(y).\, i\,(z)] + \\ & 2\pi h_{D2} [ii(x).\, i\,(y).\, i\,(z)] + 2\pi h_{D2} [x(x).\, vii\,(y).\, i\,(z)] + \\ & 2\pi h_{D2} B [ii(x).\, vii\,(y).\, ix\,(z)] + 2\pi h_{D2} B [x(x).\, vii\,(y).\, ix\,(z)] \end{aligned} \quad (8)$$

Constant B is only applicable to flow regimes that have felt the interface as one of their boundaries. Therefore, if the interface is not felt, the constant B is not included in the integrand representing the flow regime. Individual layer modification factors are represented by A and B. Factors A and B modify source functions to the layered reservoir along the z-axes for the crossflow interface. Each weighs the effect of crossflow along the z-axis on pressure response.

α is the time normalisation factor of Layer 2 responses with respect to Layer 1.

$$\alpha = \frac{t_{D1}}{t_{D2}} \quad (9)$$

2.4.3 Delineation of Flow Regimes

Determination of Intervals of Subsistence of Each Flow Regime Using Correlation

The limits of the integrals in Equations 2 and 6 represent the intervals of subsistence of each flow regime. These intervals are estimated using correlations presented by Odeh et al. (1990). The corresponding intervals for a layered reservoir are shown in Table 2.

$$P_{D1} = P_{D2} \quad (10)$$

$$\frac{\partial P_{D1}}{\partial z_D} = \frac{\partial P_{D2}}{\partial z_D} \quad (11)$$

2.4.4 Derivation of Individual Layers Modification Factors (A and B)

By applying some boundary conditions factors were derived. During crossflow, at the interface, Pressure in Layer 1 equals pressure in layer 2. Expressed in dimensional form as Equation 10. Velocity of fluid in Layer 1 equals velocity in Layer 2. Expressed in dimensionless form as Equation 11 (Owolabi *et al.,* 2012)

where M is interlayer mobility ratio. Individual layer modification factors A and B) were derived using interface condition expressed above. It is generally easy to adopt some of these factors in model for complex models. Similar approach in some common techniques (Owolabi *et al.,* 2012; Mutisya *et al.,* 2020).

3. Results and Discussion

Prior to results compilation, the model was verified based on existing literature.

3.1 Model Validation

The complexity of the model presented in this article would not allow for all-inclusive comparison with any classical literature. However, the validation was taken in parts, by comparing various parts of the model in this article with the similar model presented in other articles verification of model was accomplished. Verification was done using the data obtained from the model developed by Viana et al (Viana *et al.,* 2022) as shown in Table 3.

Table 3: Reservoir system parameters used for validation of model using Viana et al model.

Case	Properties	Layer1, Region 1
A	r(m)	16
	K(md)	1000
	h(m)	15
	μ(cp)	5.1
B	r(m)	10
	K(md)	500
	h(m)	10
	μ(cp)	3.5

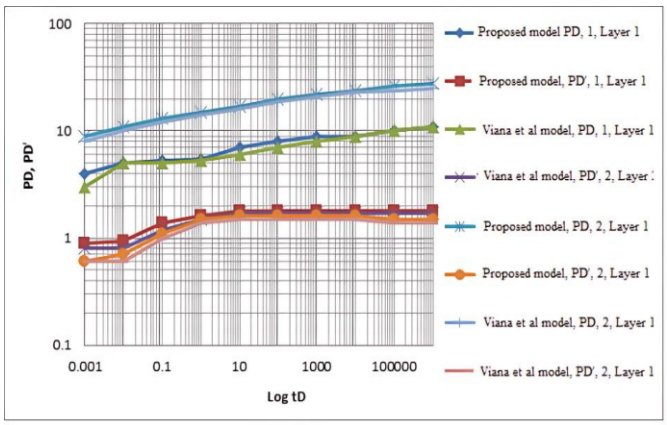

Figure 5: Log-log plot of P_D, P_D' versus t_D validation of the proposed model versus Viana et al model

As shown in Figure 5, Case A exhibited early time radial flow. Curve obtained from the proposed model compares well with Viana et al model, though higher values of P_D, P_D' were obtained at some point. The curve obtained from Case B manifested characteristic signature of flow regime 2 of the proposed model. There were points along the curve where Viana model resulted in lower values. The pressure measured at the well is directly related to the equivalent permeability (k_{eq}). The permeability value used for this work is the equivalent permeability obtained from the permeability values along the principal axes. Data and model contained in the article of Chen Li were used for further verification (Li *et al*., 2021). A large fracture conductivity factor was used so as to appropriately simulate horizontal well. The analytical solution results in this paper are compared with those in article of Li (Li *et al*., 2021). Basic data from Li's paper are listed in Table 4.

Table 4: Reservoir system parameters used for validation 2 by Li's model

Properties	Values
r(ft)	800
k(md)	26
h(ft)	6
(cp)	0.01082
rw(ft)	0.5
∅	0.01
L(ft)	200
燼g/cm^3)	1.47
C_t (psi^{-1})	0.002234
T(R)	530
P_{ic} (psia)	447.7
P_L (psi)	167.58
V_L (scf/ft^3)	18.632
(hr)	328990
z	0.94

As shown in Figure 11, Li's solution was relatively small compared with the solution from this article. Characteristic signatures of late flow period were similar to characteristic signatures obtained in a multilayered reservoir (Cobb *et al.,* 1972).

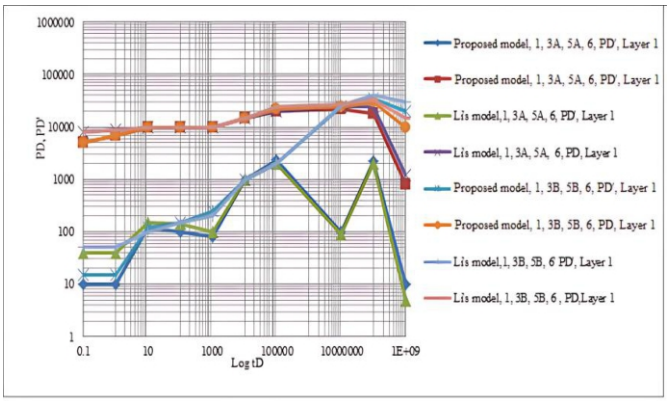

Figure 11: Comparison with the results from the proposed model and Li's model on log-log plot

With the values of input data, various flow regimes manifested, each flow regime recognized by it characteristic signature. The various flow regimes obtained from Li's model were observed to simulate some particular flow regimes, as indicated, that make up the model of this articles. Since wellbore was not considered in model of this article, that section for wellbore dominated period was overlooked. The characteristic curve of early time radial flow could be observed between time $t_D = 0.1$ and $t_D = 0.2$. Though it did not last for a long time, early time linear flow was observed between time $t_D = 0.2$ and $t_D = 1000$. Early linear flow is designated

Table 2: Interval of Flow Regimes

S/N	Start Time		End Time	
	Layer 1	Layer 2	Layer 1	Layer 2
1	0	0	t_{D1}= min. 0.132, $\frac{1.9008d_{zD1}^2}{L_{D1}^2}$, $\frac{1.7424d_{yD1}^2}{L_{D1}^2}$	t_{D1}= min. 0.132α, $\frac{1.9008\alpha d_{zD1}^2}{L_{D1}^2}$, $\frac{1.7424\alpha d_{yD1}^2}{L_{D1}^2}$
2	t_{D2}= 0.132, provided $\frac{1.9008d_{zD1}^2}{L_{D1}^2}$ & $\frac{1.7424d_{yD1}^2}{L_{D1}^2} > 0.132$	t_{D2}= *0.132, provided* $\frac{1.9008\alpha d_{zD1}^2}{L_{D1}^2}$ & $\frac{1.7424\alpha d_{yD1}^2}{L_{D1}^2} > 0.132$	t_{D3}= min. $\frac{1.9008d_{zD1}^2}{L_{D1}^2}$, $\frac{1.7424d_{yD1}^2}{L_{D1}^2}$, $2.112\left(\frac{d_{xD1}}{L_{D1}}+\frac{1}{4}\right)^2$	t_{D3}= min. $\frac{1.9008\alpha d_{zD1}^2}{L_{D1}^2}$, $\frac{1.7424\alpha d_{yD1}^2}{L_{D1}^2}$, $2.112\alpha\left(\frac{d_{xD1}}{L_{D1}}+\frac{1}{4}\right)^2$
3(a)	t_{D4}= $\frac{1.9008d_{zD1}^2}{L_{D1}^2}$,provided $\frac{1.9008d_{zD1}^2}{L_{D1}^2} <$ 0.132, $\frac{1.7424d_{yD1}^2}{L_{D1}^2}$	t_{D4}= $\frac{1.9008\alpha d_{zD1}^2}{L_{D1}^2}$,provided $\frac{1.9008\alpha d_{zD1}^2}{L_{D1}^2} < 0.132$, $\frac{1.7424\alpha d_{yD1}^2}{L_{D1}^2}$	t_{D5}= min 0.16896, $\frac{1.7424d_{yD1}^2}{L_{D1}^2}$	t_{D5}= min 0.16896α, $\frac{1.7424\alpha d_{yD1}^2}{L_{D1}^2}$
3(b)	t_{D6}= $\frac{1.7424d_{yD1}^2}{L_{D1}^2}$ provided $\frac{1.7424d_{yD1}^2}{L_{D1}^2} <$ 0.132, $\frac{1.9008d_{zD1}^2}{L_{D1}^2}$	t_{D6}= $\frac{1.7424\alpha d_{yD1}^2}{L_{D1}^2}$ provided $\frac{1.7424\alpha d_{yD1}^2}{L_{D1}^2} < 0.132$, $\frac{1.9008\alpha d_{zD1}^2}{L_{D1}^2}$	t_{D7}= min 0.16896, $\frac{1.9008d_{zD1}^2}{L_{D1}^2}$	t_{D7}= min 0.16896α, $\frac{1.9008\alpha d_{zD1}^2}{L_{D1}^2}$
4(a)	t_{D8}= 1.56288	t_{D8}= 1.56288α	t_{D9}= min$\frac{1.7424d_{yD1}^2}{L_{D1}^2}$, $2.112\left(\frac{d_{xD1}}{L_{D1}}+\frac{1}{4}\right)^2$	t_{D9}= min. $\frac{1.7424\alpha d_{yD1}^2}{L_{D1}^2}$, $2.112\alpha\left(\frac{d_{xD1}}{L_{D1}}+\frac{1}{4}\right)^2$
4(b)	t_{D8}= 1.56288	t_{D8}= 1.56288α	t_{D10}= min.$\frac{1.9008d_{zD1}^2}{L_{D1}^2}$, $2.112\left(\frac{d_{xD1}}{L_{D1}}+\frac{1}{4}\right)^2$	t_{D10}= min$\frac{1.9008\alpha d_{zD1}^2}{L_{D1}^2}$, $2.112\alpha\left(\frac{d_{xD1}}{L_{D1}}+\frac{1}{4}\right)^2$
4(c)	t_{D8}= 1.56288	t_{D8}= 1.56288α	t_{D11}= min $\frac{1.9008d_{zD1}^2}{L_{D1}^2}$, $\frac{1.7424d_{yD1}^2}{L_{D1}^2}$	t_{D11}= min $\frac{1.9008\alpha d_{zD1}^2}{L_{D1}^2}$, $\frac{1.7424\alpha d_{yD1}^2}{L_{D1}^2}$
5(a)	t_{D12}= min. $\frac{1.9008d_{zD1}^2}{L_{D1}^2}$, $5.068\left(\frac{d_{xD1}}{L_{D1}}+\frac{1}{4}\right)^2$	t_{D12}= min. $\frac{1.9008\alpha d_{zD1}^2}{L_{D1}^2}$, $5.068\alpha\left(\frac{d_{xD1}}{L_{D1}}+\frac{1}{4}\right)^2$	t_{D13}= $\frac{1.7424d_{yD1}^2}{L_{D1}^2}$	t_{D13}= $\frac{1.7424\alpha d_{yD1}^2}{L_{D1}^2}$
5(b)	t_{D14}= min. $\frac{1.7424d_{yD1}^2}{L_{D1}^2}$, $5.068\left(\frac{d_{xD1}}{L_{D1}}+\frac{1}{4}\right)^2$	t_{D14}= min. $\frac{1.7424\alpha d_{yD1}^2}{L_{D1}^2}$, $5.068\alpha\left(\frac{d_{xD1}}{L_{D1}}+\frac{1}{4}\right)^2$	t_{D15}= $\frac{1.9008d_{zD1}^2}{L_{D1}^2}$	t_{D15}= $\frac{1.9008\alpha d_{zD1}^2}{L_{D1}^2}$
5(c)	t_{D16}= min. $\frac{1.7424d_{yD1}^2}{L_{D1}^2}$, $\frac{1.9008d_{zD1}^2}{L_{D1}^2}$	t_{D16}= min. $\frac{1.7424\alpha d_{yD1}^2}{L_{D1}^2}$, $\frac{1.9008\alpha d_{zD1}^2}{L_{D1}^2}$	t_{D17} = $5.068\left(\frac{d_{xD1}}{L_{D1}}+\frac{1}{4}\right)^2$	t_{D17} = $5.068\alpha\left(\frac{d_{xD1}}{L_{D1}}+\frac{1}{4}\right)^2$
6	t_{D18} = max. $\frac{1.7424d_{yD1}^2}{L_{D1}^2}$, $\frac{1.9008d_{zD1}^2}{L_{D1}^2}$, $5.068\left(\frac{d_{xD1}}{L_{D1}}+\frac{1}{4}\right)^2$	t_{D18} = max. $\frac{1.7424\alpha d_{yD1}^2}{L_{D1}^2}$, $\frac{1.9008\alpha d_{zD1}^2}{L_{D1}^2}$, $5.068\alpha\left(\frac{d_{xD1}}{L_{D1}}+\frac{1}{4}\right)^2$	t_D	αt_D

*min. implies "minimum of", *max. implies "maximum of"

as 3B. Flow regime 3B can be distinguished by the straightening of curve of P_D and the declining of P_D', the duration of this stage always short. Sometimes, it was concealed by the wellbore storage stage or early time linear flow. In contrast, flow regime 3A can be distinguished by the gentle slopping of P_D and rapidly increasing of P_D'. The direction of flow relative to the direction of the well is perpendicular to the direction of the well in the horizontal plane. No flow boundary was encountered. Similar trends were observed in literature (Shahrian *et al.,* 2022).
Further verification done with Viana et al model (Viana *et al.,* 2022), data used are as shown in Table 5. The effect cross flow was exposed.

Table 5: Reservoir system parameters used for validation 3 of model using Viana et al model

Case	Properties	Layer1, Region 1	Layer2, Region 1
D1	r(m)	15	15
	K1(md)	300	3000
	K2(md)	5	2.5
	h(m)	15	15
	(cp)	5.1	
D2	r(m)	15	15
	K1(md)	500	3000
	K2(md)	5	2.5
	h(m)	15	15
	(cp)	5.1	

Considering formation crossflow as shown in Figure 12, curves obtained from Case D1 march well with flow regime 1, 3B and 4A. While curves obtained from Case D2 march well with flow regime 1, 3B and 4C. shows the graph results for the pressure. P_D values obtained from model of this article was observed to be higher than those obtained from Viana et al. However, close match was observed between the two models. Due to presence of crossflow after t_D =1, P_D for Case D1 was shown to increase slightly with time, while P_D' started to slope downwards. But for Case D2 where there was no crossflow after t_D =1, P_D was shown to increase gradually with time, while P_D' continue to be straight horizontally, indicating early radial flow when no boundary has been felt. The effect of crossflow was manifested as a steady state behavior as shown also by Viana et al. (Viana *et al.,* 2022). However, after t_D = 100, P_D' of his model for Case 2 was observed to be sloping upwards increasingly, indicating that effect of no crossflow boundary has become effective. Such behavior is expected because flow regime 4C depict flow along y and z-axes given that no crossflow boundary x-axis has been felt.

3.2 Pressure response of layered bounded reservoir produced by horizontal wells
It is a common practice to model layered reservoirs as a single compartment by averaging the reservoir parameters associated with each reservoir layer. However, this practice is inadequate as it pressure of each layer changes independently. Change in pressure from each layer affect the entire performance of the reservoir. It may lead to inter-layer flow, fluid by-pass, and premature depletion of a particular layer. Understanding reservoir performance requires knowledge of permeability and skin factor of each layer (Shahrian *et al*., 2021). When considering the effect of layering properties of each layer should be different. Factors such as and M were used. For crossflow interface, factors A and B were incorporated.

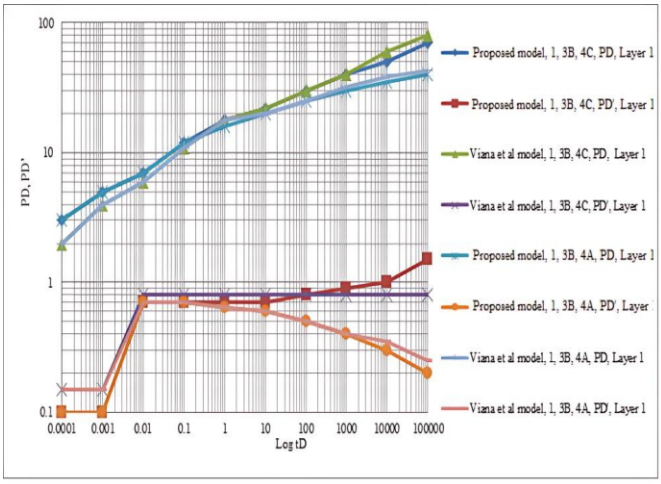

Figure 12: Comparison with the results from the proposed model and Viana's model for crossflow and no crossflow on log-log plot.

3.3 Description of each possible flow regime and conditions that necessitate their existence
For the set of data considered, the flow regime that subsisted and their intervals depend on the reservoir system parameters. It was also observed that some flow regimes cannot co-exist. In some instances, where two consecutive flow regime overlap, i.e. another flow regime starts when other has not fully died down, only the fully established was shown since the other was masked. When the value of factors is not unity effect of layering was observed. In such case . Otherwise, when it means there is no layering. As soon as there is crossflow, =1he pressure declines and tends to zero. Hence, subsequent flow regimes are masked.
1. When the flow is along y, z – axes but along the x-axis flow is confined within the well. Early radial flow regime around the well length was observed, provided flow has not gone beyond tip of well. Within this period, flow along x – axis is not affected by time as flow is still within the well. It stops when flow goes beyond well or when any external boundary, other than x-axis, is felt. The dimensionless pressure rises moderately with respect to dimensionless time. The slope of the log –log plot for the pressure derivative is constant.
2. Flow along x, y, z –axes. Starts if flow initially along y and z axis but confined within the well goes beyond the tips of the well. It implies that there is sufficient time for flow to go beyond the tips of the well before any boundary is felt. This type of flow is a spherical flow regime. It occurs if well length is short compared to layer thickness. The dimensionless pressure rises very sluggishly with time while the dimensionless pressure derivative rises very sluggishly with time. It can be used as symptomatic tool to suggest the need to extend producing well length. Deviated well completion may also offer good alternative.
3. (a) Flow along y – axis. It occurs when the interface or top or bottom boundary has been felt. It occurs if the reservoir thickness is low compared with other dimensions of the reservoir. The dimensionless pressure is tends to straighten horizontally, while the dimensionless pressure derivative declines rapidly and tends towards zero thus indicating external energy.
(b) Flow along z – axis. It occurs when the boundary along y –axis is felt before either the interface or top or bottom boundary is felt. It is possible when reservoir extent is closer along y – axis than either the interface or top or bottom boundary. In 3a and 3b, early time linear flow is observed. It obliterates spherical flow if it occurred.
4. (a) Flow along x, y –axes, (given 3a). The flow pattern is radial at the top and bottom of well. The dimensionless pressure is tends to straighten horizontally, while the dimensionless pressure derivative declines rapidly and tends towards zero thus indicating external energy..
(b) Flow along x, z – axis, (given 3b). This is Pseudo radial flow regime. The flow pattern is radial at the tips or at the sides of the well. It is Pseudo radial flow regime. It is not as the real radial flow observed since boundary effect has commenced.
(c) Flow along y, z – axis, (given 2). This is given Pseudo radial flow regime. The flow pattern is radial at the top or at the sides of the well. It is pseudo radial flow regime. It is not as the real radial flow observed since boundary effect has commenced.
5. (a) Flow along y –axis, (given 4a or 4c). The flow is late time linear flow. The dimensionless pressure is tends to straighten horizontally, while the dimensionless pressure derivative declines rapidly and tends towards zero thus indicating external energy.
(b) Flow along z – axis (given 4b or 4c). The flow is late time linear flow. The dimensionless pressure and its rises rapidly indicating completely sealed reservoir.
(c) Flow along x – axis (given 4a or 4b). At least boundaries along two axes have been felt. Another linear flow, late time linear flow, is observed. The dimensionless pressure and its rises rapidly indicating completely sealed reservoir.
6. All boundary felt. This is a complete linear flow regime. The dimensionless pressure and its rises rapidly indicating completely sealed reservoir. The pressure decline is proportional to the rate of depletion. It signals end of economic life of well.
Results show that when the layer factors are zero, the reservoir behaves as single compartment reservoir. Pressure response was observed to increase steadily. But for other values, effect of layering is exhibited.

3.4 Identification of Layered and single compartment Reservoir
When the value of factors is not unity effect of layering was observed. In such case $\alpha \neq 1$. Otherwise, when it means there is no layering. Such reservoir is single compartment. As soon as there is crossflow, $M \neq 1$, the dimensionless pressure derivative starts to declines and tends to zero, while dimensionless pressure straightens horizontally. During crossflow from the other layer, there is maintenance of pressure in the producing layer. Hence, subsequent flow regime are masked. It is necessary to note that, there may be layering without crossflow. In such case, $\alpha \neq 1$, but $M = 0$. For layering with crossflow, the condition that must be met is that, $\alpha \neq 1$ and $M \neq 1$. The rule is that M can only exist given but the reverse is an exception. when $\alpha \neq 1, M \neq 1$.

4. Conclusion

The mathematical model presented uses the correlation for delineating flow regimes. Therefore, the number of flow regimes; type of flow regime and the interval of subsistence are determined by the reservoir system parameters. Other features of this model are:

(I) Far-reaching pressure distribution model of a two-layered bounded reservoir has been developed. In a flow period, it is not possible to have all the possible flow regimes, some will not exist depending on the reservoir system parameters, architecture of the reservoir system and the fluid properties. Also, preceding flow regimes also determines the type that may follow.

Therefore, unlike in most models in which the author decides the flow regime that occurs, the flow regime that may occur and the duration of existence is determined by the values of parameters, geometry of reservoir, fluid properties and well architecture selected.

(ii) Model was seen to produce series of radial and linear flow along the individual principal axes or combinations of any of the three principal axes. Each flow regime could be recognized by its characteristic signature in the log-log graph plots of the pressure, pressure derivative versus time.

(iii) Although, initially the permeability along the principal axes were determined ($k_x > k_y > k_z$) for easy understanding; the imposition of assumption was relax during derivation of model.

The order can change depending on the choice of parameters along any of the axes. Similarly, the imposition of layering on the reservoir can be relaxed to single compartment reservoir by choosing parameters in the layers to be the same. Such is the flexibility of the model in this article.

(iv) Correlation for delineating interval of flow regime in a single compartment reservoir has been extended to layered reservoir.

The interval of existence depends on the reservoir system parameters. Existence of some flow regimes obliterates other flow regimes. Also, when the interval of subsistence is short, the flow regime is masked and not observed.

Nomenclature

$$t_D = \frac{0.001056kt}{\phi\mu C_t L^2} \quad (12)$$

$$k = \sqrt[3]{k_x k_y k_z} \quad (13)$$

$$L_D = \frac{L}{2h}\sqrt{\frac{k}{k_z}} \quad (14)$$

$$x_D = \frac{2x}{L}\sqrt{\frac{k}{k_x}} \quad (15)$$

$$x_{eD} = \frac{2x_e}{L}\sqrt{\frac{k}{k_x}} \quad (16)$$

$$x_{wD} = \frac{2x_w}{L}\sqrt{\frac{k}{k_x}} \quad (17)$$

$$y_D = \frac{2y}{L}\sqrt{\frac{k}{k_y}} \quad (18)$$

$$y_{eD} = \frac{2y_e}{L}\sqrt{\frac{k}{k_y}} \quad (19)$$

$$y_{wD} = \frac{2y_w}{L}\sqrt{\frac{k}{k_y}} \quad (20)$$

$$z_D = \frac{2z}{L}\sqrt{\frac{k}{k_z}} \quad (21)$$

$$z_{eD} = \frac{2z_e}{L}\sqrt{\frac{k}{k_z}} \quad (22)$$

$$z_{wD} = \frac{2z_w}{L}\sqrt{\frac{k}{k_z}} \quad (23)$$

$$d_x = D_x = \frac{Xe - L}{2} \quad (24)$$

$$r_{weq} = \left[\left(\frac{k}{k_z}\right)^{0.25} + \left(\frac{k_x}{k}\right)^{0.25}\right] \quad (25)$$

$$r_{wD} = \frac{2r_{weq}}{2} \quad (26)$$

$$P_D = \frac{kh\Delta P}{141.2q\mu B_0} \quad (27)$$

References

A1 Rbeawi S. and Tiab D. (2013). Transient Pressure of Horizontal Wells in a Multi-Boundary System' American Journal of Engineering Research, 2(4), 44-66.

Adewole, E.S.,(2012). Theoretical Dimensionless Breakthrough Time of a Horizontal Well in a Two-Layered Reservoir System with Varying Architecture Part II: Letter B Architecture, Bottom Water Drive Mechanism", Advanced Materials Research, 367, 385-392. doi: 10.4028/www.scientific.net/AMR.367.385.

Afagwu C., Abubakar 1. , Kalam S., Al-Afnan S. F. , Awotunde A. A.(2020). Pressure-transient analysis in shale gas reservoirs: A review. Journal of Natural Gas Science and Engineering, 78, 103319.

Chen Z., Liao X., Xiaoliang Zhao, Xiangji Dou, Langtao Zhu (2016). A semi-analytical mathematical model for transient pressure behavior of multiple fractured vertical well in coal reservoirs incorporating with diffusion, adsorption, and stress-sensitivity. Journal of Natural Gas Science and Engineering, 29, 570-582. https://doi.org/10.1016/j.jngse.2015.08.043

Chu H., Liao X., Chen Z., Zhao X., Liu W., Dong P. (2019). Transient pressure analysis of a horizontal well with multiple, arbitrarily shaped horizontal fractures. Journal of Petroleum Science and Engineering journal. https://doi.org/10.1016/j.petrol.2019.06.003

Cobb WM, Ramey H Jr, Miller FG et al (1972) Well-test analysis for wells producing commingled zones. Journal of Petroleum Technology, 24(1), 27–37

Gringarten A.C., and Ramey H.J.J r, (1973). The use of Source and Green's Functions in solving Unsteady-flow Problems in Reservoirs. Society of Petroleum Engineers Journal, 13, 285-296.

Li C. (2021). Production Analysis for Fractured Vertical Well in Coal Seam Reservoirs with Stimulated Reservoir Volume. Hindawi Geofluids, 2021, 1864734, 12. https://doi.org/10.1155/2021/1864734

Lu J., Rahman M. M., Yang E., Alhamami M. T., Zhong H. (2021). Pressure transient behavior in a multilayer reservoir with formation crossflow. Journal of Petroleum Science and Engineering, 208(b). https://doi.org/10.1016/j.petrol.2021.109376.

Mutisya M. P., Adewole E. S., Kennedy A., Otieno and Okang O. D. A (2020). Mathematical Model for Pressure Distribution in a Bounded Oil Reservoir Subject to Single-Edged and Bottom Constant Pressure. IOSR Journal of Mathematics. 16(4) 24-30.

Odeh A. S. and Babu D.K. (1990): Transient Flow Behavior of Horizontal Wells: Pressure Drawdown and Buildup Analysis 'SPE Formation Evaluation, March, 10-14.

Oloro J., Adewole E.S.And Olafuyi O.A., (2012). 'Pressure Distribution of Horizontal Wells in a Layered Reservoir with Simultaneous Gas Cap and Bottom Water Drives' American Journal of Engineering Research, 3(12), 41-53

Owolabi A.F., Olafuyi O.A., Adewole E.S. (2012). Pressure Distribution an a Layered Reservoir with Gas-Cap and Bottom Water. Nigerian Journal of Technology, 31(2), 189-198.

Shahrian E., and Masihi M. (2021) Analysis of well testing results for single phase flow in reservoirs with percolation structure. Oil & Gas Science and Technology – Rev. IFP Energies nouvelles 76, 15. https://doi.org/10.2516/ogst/2020092

Viana I., Bela R. V., Pesco S., Barreto A. Junior, (2022). An analytical model for pressure behavior in multilayered radially composite reservoir with formation crossflow. Journal of Petroleum Exploration and Production Technology https://doi.org/10.1007/s13202-022-01460-x

Wang J., Wang X., Dong W. (2017). Rate decline curves analysis of multiple-fractured horizontal wells in heterogeneous reservoirs. Journal of Hydrology. 55, 527-539. https://doi.org/10.1016/j.jhydrol.2017.08.024

Appendix 1

Basic instantaneous source functions (Gringarten & Ramey, 1973)

X=0 X_W X_e	Source	Function number	Source function
	infinite plane source	i(x)	$\frac{exp\left[-\frac{(x-x_w)^2}{4n_x t}\right]}{\sqrt[2]{n_x t}}$
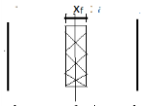	infinite slab source	ii(x)	$\frac{1}{2}\left[erf\frac{\frac{x_f}{2}+(x-x_w)}{\sqrt[2]{n_x t}}+erf\frac{\frac{x_f}{2}-(x-x_w)}{\sqrt[2]{n_x t}}\right]$
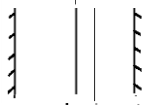	prescribed flux, plane source	vii(x)	$\frac{1}{x_e}\left[1+2\sum_{n=1}^{\infty}exp\left(-\frac{n^2\pi^2 n_x t}{x_e^2}\right)cos\frac{n\pi x_w}{x_e}cos\frac{n\pi x}{x_e}\right]$
	mixed boundary, plane source	ix(x)	$\frac{2}{x_e}\sum_{n=1}^{\infty}exp\left(-\frac{(2n+1)^2\pi^2 n_x t}{4x_e^2}\right)cos\frac{(2n+1)\pi x_w}{x_e}cos\frac{(2n+1)\pi x}{x_e}$
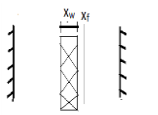	prescribed flux, slab source	x(x)	$\frac{x_f}{x_e}\left[1+\frac{4x_e}{\pi x_f}\sum_{n=1}^{\infty}\frac{1}{n}exp\left(-\frac{n^2\pi^2 n_x t}{x_e^2}\right)sin\frac{n\pi x_f}{2x_e}cos\frac{n\pi x_w}{x_e}cos\frac{n\pi x}{x_e}\right]$

Appendix 2

Extension of Source and Greens Function Table. For the case prescribed pressure at x=0 and prescribed flux at x=0. This is a lateral inversion of ix (z). Modified form of ix (x), is given as ix (x)'

X=0 X_W X_e	Source	Function number	Source function
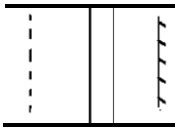	mixed boundary, plane source	ix(x)'	$\frac{2}{x_e}\sum_{n=1}^{\infty}exp\left(-\frac{(2n-1)^2\pi^2 n_x t}{4x_e^2}\right)sin\frac{(2n-1)\pi x_w}{x_e}sin\frac{(2n-1)\pi x}{x_e}$